

Journal of Chemical, Biological and Physical Sciences



An International Peer Review E-3 Journal of Sciences

Available online at www.jcbps.org

Section C: Physical Sciences

CODEN (USA): JCBPAT

Research Article

Preparation and Study of Some Physical Properties of $\text{Cu}_x\text{Zn}_{1-x}\text{S}$ Thin Films

Nabeel A. Bakr*, Asaad A. Kamil, Maryam S. Jabbar

Department of Physics, College of Science, University of Diyala, Diyala, Iraq

Received: 01 January 2017; Revised: 10 January 2018; Accepted: 18 January 2018

Abstract: In this study, $\text{Cu}_x\text{Zn}_{1-x}\text{S}$ (where $x = 0, 0.1, 0.3, 0.5, 0.7, 0.9$ and 1) thin films have been successfully deposited on glass substrates by chemical spray pyrolysis (CSP) technique at substrate temperature of ($400\text{ }^\circ\text{C}$). The thickness of the prepared thin films was about (350 ± 30) nm measured by gravimetric method. Various characterization techniques have been used to investigate the structural and optical properties of the prepared thin films. The XRD results showed that the CuS film has a polycrystalline nature with covellite-hexagonal structure and preferred orientation along (103) plane, and the ZnS film has a polycrystalline wurtzite-hexagonal structure with preferred orientation along (0010) plane, while the thin films prepared with different mixing ratios have a polycrystalline structure and mixture phases of covellite-hexagonal and wurtzite-hexagonal. AFM results showed homogenous and smooth thin films. FESEM results showed the formation nanostructures with different shapes, such as cauliflower, semi-spherical, hexagonal, and in the form of plates and rods. The UV-Visible-NIR absorbance spectra were recorded in the range of (350-900) nm to investigate the optical characteristics. The results have shown that the transmittance of the prepared thin films decreases with increasing the CuS ratio and the absorption coefficient value is ($\alpha > 10^4\text{ cm}^{-1}$) for all prepared thin films, which this in turn proved that the prepared thin films are likely to have direct electronic transitions. It is found that the optical energy gap decreases with increasing the CuS ratio, and it is in the range of (2.12-3.34) eV.

Keywords: $\text{Cu}_x\text{Zn}_{1-x}\text{S}$, Structural Properties, Optical Properties, Nanostructures

1. INTRODUCTION

Copper sulfide (Cu_xS , $x = 1-2$) belongs to I-VI group compounds which is one of the most interesting materials, for it has semiconducting properties and exists in several crystallographic and stoichiometric forms. Owing to its electrical conductivity and optical band gap, it is mainly used in solar cell applications¹. Based on various parameters, copper sulfide exhibits different crystallographic orientation. Copper sulfide is found to exist in two forms: "copper rich phase" and "copper poor phase". They are chalcocite (Cu_2S), djurlite ($\text{Cu}_{1.96}\text{S}$), digenite ($\text{Cu}_{1.8}\text{S}$), anilite ($\text{Cu}_{1.75}\text{S}$) and covellite (CuS). Out of all these stoichiometric forms, covellite comes under copper poor phase². The covellite form of CuS thin films shows metallic-like electrical conductivity and possesses near-ideal solar control characteristics. The direct band gap of this material reported in the literature lies in the range³ from (1.2 to 3) eV.

The CuS thin films have been deposited by various methods such as chemical vapor deposition⁴, successive ionic layer adsorption and reaction (SILAR) method⁵, chemical bath deposition (CBD)⁶, microwave assisted chemical bath deposition (MA-CBD)⁷ and chemical vapor reaction⁸, etc. On the other hand, ZnS belongs to II-VI group of compound semiconductors with energy band gap of about 3.7 eV in the bulk form. This wide band gap, which is even greater than ZnO (3.4 eV) and GaN (3.4 eV), makes it highly suitable for visible-blind ultraviolet photodetectors.

It also has several other potential applications such as electroluminescence devices and buffer layer for solar cells⁹, etc. ZnS has been deposited by various techniques such as molecular beam epitaxy¹⁰, MOCVD¹¹, chemical bath deposition¹², and pulsed electrodeposition¹³ etc. In the present study, $\text{Cu}_x\text{Zn}_{1-x}\text{S}$ (where $x = 0, 0.1, 0.3, 0.5, 0.7, 0.9$ and 1) thin films are deposited by chemical spray pyrolysis method at 400°C. The films are characterized by X-ray diffraction (XRD), AFM, FESEM and UV-Vis-NIR spectroscopy and the results were discussed to investigate their possible applications.

2. EXPERIMENTAL DETAILS

$\text{Cu}_x\text{Zn}_{1-x}\text{S}$ (where $x = 0, 0.1, 0.3, 0.5, 0.7, 0.9$ and 1) thin films were deposited on glass substrates (Soda lime glass) using a homemade chemical spray pyrolysis system. Two precursor solutions were prepared using distilled water as a solvent. The first solution was prepared by mixing equal volumes of (0.1 M) of $\text{Cu}(\text{CH}_3\text{COO})_2 \cdot \text{H}_2\text{O}$ (from Alpha Chemika - India) solution with (0.1 M) of $\text{SC}(\text{NH}_2)_2$ (from Central Drug House (P) Ltd. - India) solution. While, the second solution was prepared by mixing equal volumes of (0.1 M) of $\text{Zn}(\text{CH}_3\text{COO})_2 \cdot 2\text{H}_2\text{O}$ (from Scharlau Chemicals - Spain) solution with (0.1 M) of $\text{SC}(\text{NH}_2)_2$ solution. The final solution was prepared by mixing appropriate ratios ($x = 0, 0.1, 0.3, 0.5, 0.7, 0.9$, and 1) of the first and second solutions.

All aqueous solutions were magnetically stirred for 10 min, and then the resultant solutions were sprayed on glass substrates ($2.5 \times 2.5 \text{ cm}^2$) which were kept at temperature of 400 °C. The thickness of the prepared thin films was about $(350 \pm 30) \text{ nm}$ measured by gravimetric method. Other deposition conditions such as spray nozzle substrate distance (30 cm), spray time (10 s), spray interval (2 min) and pressure of the carrier gas (1.5 bar) were kept constant during the deposition process. The prepared films were characterized by X-ray diffraction (Bruker D8 Advance, $\text{CuK}\alpha$ line, 1.54056 Å), Atomic Force Microscopy (AFM) using scanning probe microscope type (SPM- AA3000, Contact mode, supplied by Angstrom, Advanced Inc.), Field Emission Scanning Electron Microscopy (FESEM) (MIRA3, TE-SCAN) and UV-VIS-NIR spectrophotometer (Shimadzu, UV- 1800).

3. RESULTS AND DISCUSSION

3.1 X-ray diffraction analysis: Figure (1) shows the X-ray diffraction patterns of $\text{Cu}_x\text{Zn}_{1-x}\text{S}$ (where $x=0, 0.1, 0.3, 0.5, 0.7, 0.9$ and 1) thin films. It can be observed that the positions of the XRD peaks of CuS film are located at angles ($2\theta \sim 29.28^\circ, 31.78^\circ, 32.84^\circ, 47.82^\circ$ and 59.4°) corresponding to the planes (102), (103), (006), (107) and (116) respectively, which belong to the covellite-hexagonal structure with the preferred orientation of (103). These peaks are consistent with the International Center for Diffraction Data (ICDD) card number (06-0464). The appearance of several peaks in the XRD pattern indicates that the films have a polycrystalline structure. These results are in agreement with the results reported by other studies^{7,14}. From the same figure, it can be noticed that the peaks positions of the ZnS film are located at angles ($2\theta \sim 28.6^\circ, 47.76^\circ$ and 56.6°) corresponding to the planes (0010), (110) and (1110) respectively, which are attributed to the wurtzite-hexagonal structure with the preferred orientation of (0010). These results are in agreement with the International Center for Diffraction Data (ICDD) card number (12-0688) and are similar to the reported ones by other studies^{15,16}. From the same figure, we notice that other films prepared with different mixing ratios have a polycrystalline structure, where the XRD peaks of the samples of $x = 0.9$ and 0.7 belong to the hexagonal phase of (CuS) assigned by the (+) symbol, while the XRD peaks of the samples of $x = 0.5, 0.3$ and 0.1 belong to mixture phases of the hexagonal phase of CuS assigned by the (+) symbol, and the hexagonal phase of ZnS assigned by the (*) symbol. We also notice from the figure that the highest number of peaks appear in the sample of $x = 0.5$ ($\text{Cu}_{0.5}\text{Zn}_{0.5}\text{S}$) film, which means the formation of more than one phase of the CuS material and ZnS material at the same time. It is also clear that the increase in the intensity of the peaks is due to the increase of CuS ratio, where the CuS phase becomes dominant resulting to the formation of larger crystals and reduction of crystalline defects and orientation to the preferred orientation of the CuS compound¹⁷.

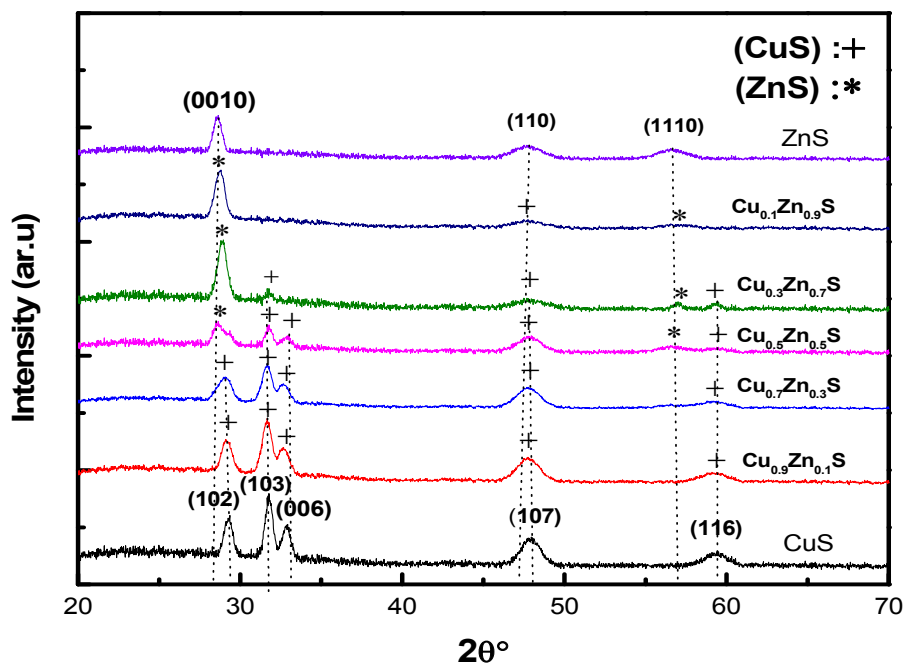


Fig. (1): X-ray diffraction patterns of $\text{Cu}_x\text{Zn}_{1-x}\text{S}$ thin films.

The interplanar spacing (d) was calculated using Bragg's equation⁹:

$$2d\sin\theta = n\lambda \quad (1)$$

For hexagonal lattice, the lattice constants (a_o , c_o) are given by¹⁸:

$$\frac{1}{d^2} = \frac{4}{3} \left(\frac{h^2 + hk + k^2}{a_o^2} \right) + \frac{l^2}{c_o^2} \quad (2)$$

Where (h , k , l) are the Miller indices. From **Table (1)**, it is clear that the values of the lattice constants of CuS and ZnS film are in agreement with the values of the (ICDD) standard cards for both materials ($a_o = 3.792 \text{ \AA}$, $c_o = 16.34 \text{ \AA}$) and ($a_o = 3.82 \text{ \AA}$, $c_o = 31.20 \text{ \AA}$) respectively. From the same table, it can be observed also that the values of the lattice constants of the thin films prepared with different mixing ratios are shifted from their values of CuS and ZnS films and from their values in the (ICDD) standard cards. This deviation is due to the replacement of the two compounds ions with each other, since the diameter of copper ions is (0.73 \AA), which is greater than the diameter of zinc ions (0.60 \AA)¹⁶.

Table (1): Structural parameters of $\text{Cu}_x\text{Zn}_{1-x}\text{S}$ thin films.

X value	1 (CuS)	0.9	0.7	0.5	0.3	0.1	0 (ZnS)
hkl	103	103	103	103	0010	0010	0010
2θ (deg)	31.78	31.8	31.8	31.8	28.8	28.7	28.6
d_{hkl} (Å)	2.8143	2.8122	2.8122	2.8122	3.0984	3.1084	3.1198
FWHM (deg)	0.5882	0.6858	0.7154	0.5303	0.7128	0.7136	0.5876
Lattice constant (a_o) (Å)	3.795	3.87	3.87	3.77	3.799	3.798	3.818
Lattice constant (c_o) (Å)	16.34	15.80	15.80	16.37	30.98	31.09	31.20
D (nm)	14.05	12.05	11.55	15.58	11.51	11.49	13.95
T_c (hkl)	0.81	1.62	1.75	1.91	1.06	1.28	0.94

The crystallite size of the prepared thin films was calculated by Scherrer's formula given by the following equation³:

$$D = 0.94 \lambda / (\beta \cos\theta) \quad (3)$$

Where D is the crystallite size, λ is the X-ray wavelength of $\text{CuK}\alpha$ line radiation, β is the full width at half maximum (FWHM) and θ is the Bragg's angle. **Table (1)** shows that the crystalline size values change unsystematically, this is due to phase change between the hexagonal phases of CuS and ZnS compound. The highest value of the crystallite size is for ($\text{Cu}_{0.5}\text{Zn}_{0.5}\text{S}$) film with value of (15.58 nm).

The texture coefficients $T_{c(hkl)}$ for all samples have been calculated from the X-ray data using the well-known formula¹⁹:

$$T_c = \frac{I_{(hkl)}/I_{o(hkl)}}{N^{-1} \sum_N I_{(hkl)}/I_{o(hkl)}} \quad (4)$$

Where $I_{(hkl)}$ is the measured intensity, $I_{o(hkl)}$ taken from the JCPDS data, (Nr) is the reflection number and (hkl) is Miller indices. The texture coefficient is calculated for crystal plane (103) and (0010) of

the prepared thin films. Its values for CuS and ZnS films are less than one, which indicates that there are more than one preferred orientation, whereas its values for other thin films prepared with different mixing ratios are greater than one, which indicates that the crystal growth of the thin films are within the preferred orientations (103) and (0010) only. All these results are shown in **Table (1)**.

3.2 AFM analysis: The surface morphology of the thin films deposited on glass substrates is carried out using AFM. The size of scanned area was $(2 \times 2) \mu\text{m}^2$. **Figure (2)** shows uniform and homogeneous surface with pinholes and having a large number of grains. The grain size of thin films is in the range of several tens of nanometers which indicates the crystalline nature of the films. The average roughness value, the grain size and root mean square roughness of all films are shown in **Table (2)**. From the table, it can be noticed that the values of the average roughness, the grain size, and root mean square roughness change unsystematically, and the ZnS film has maximum value of the surface roughness, root mean square roughness and the grain size as well.

Table (2): Average roughness, root mean square roughness, and grain size of $\text{Cu}_x\text{Zn}_{1-x}\text{S}$ thin films.

x value of $\text{Cu}_x\text{Zn}_{1-x}\text{S}$	Average Roughness (nm)	RMS (nm)	Grain Size (nm)
1 (CuS)	11.7	13.5	68.73
0.9	0.356	0.422	97.46
0.7	1.64	1.97	90.02
0.5	4.36	5	95.68
0.3	2.92	3.38	95.02
0.1	1.62	1.91	73.15
0 (ZnS)	15.3	17.8	103.78

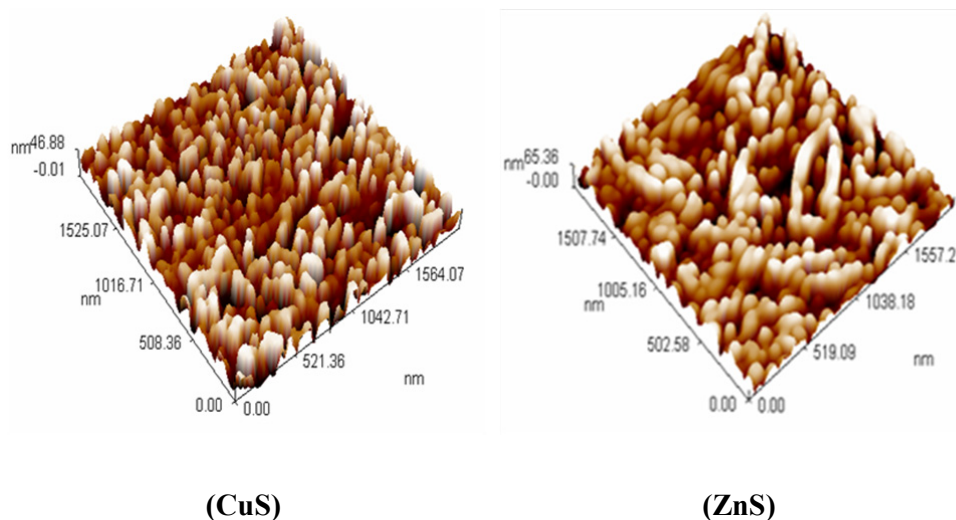


Fig. (2a): 3-D AFM images of CuS and ZnS thin films.

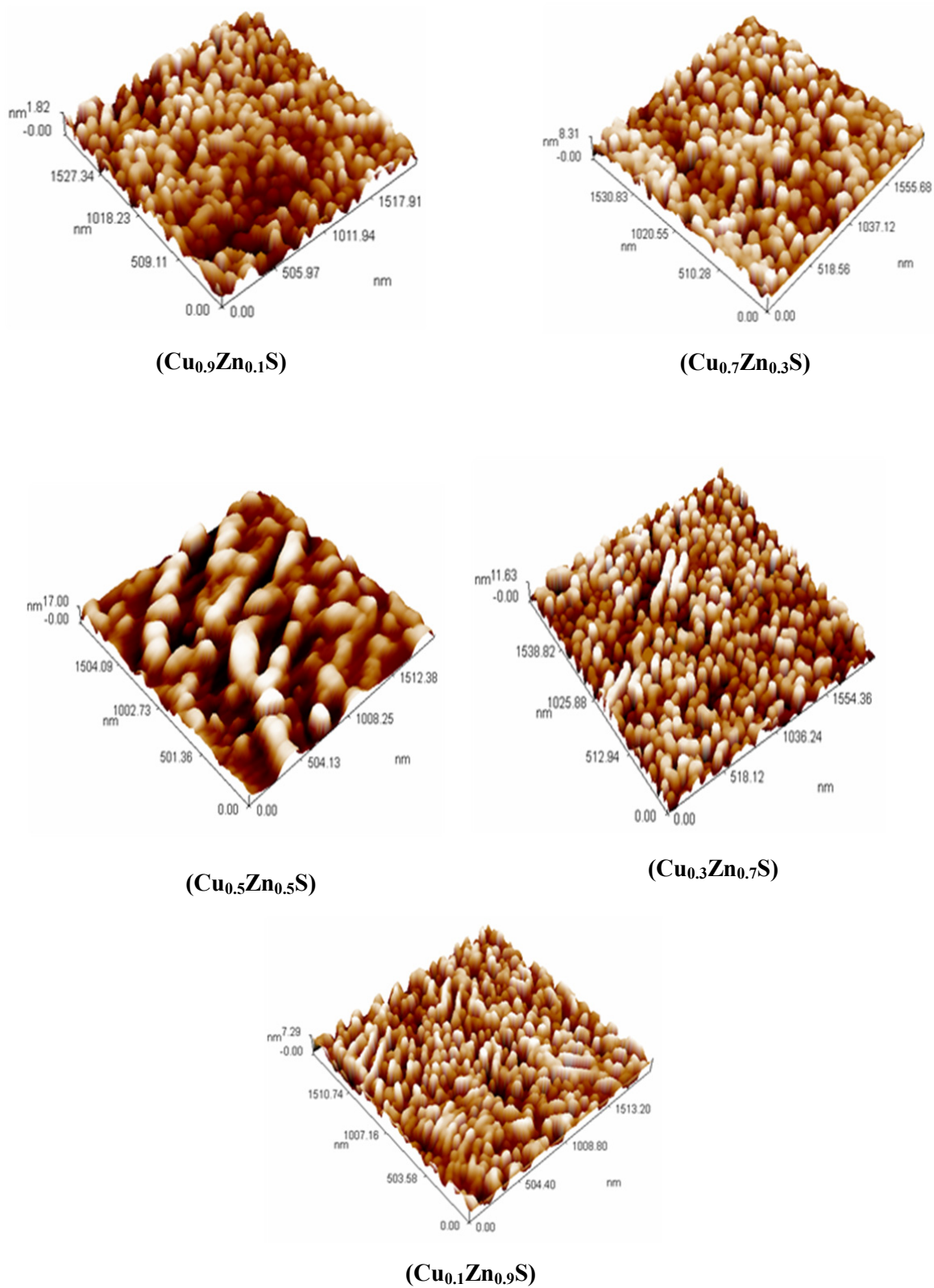


Fig. (2b): 3-D AFM images of $\text{Cu}_x\text{Zn}_{1-x}\text{S}$ (where $x=0.9, 0.7, 0.5, 0.3$ and 0.1) thin films.

3.3 FESEM analysis: The surface topography of the deposited material of the prepared thin films was studied using (FESEM), which scans the surfaces with high magnification and high precision. The images of all films with magnification of (100KX) are shown in **Figures (3a)** and **(3b)**. From **Figure (3a)**, it is observed that the CuS film grew in the form of cauliflower-like and semi-spherical nanostructures, these structures are composed of many packed grains, and the appearance of large scale grains on the surface of the film can be clearly seen, while the image of the ZnS film shows the formation of nanostructures in the form of plates and rods packed and arranged above each other. From **Figure (3b)**, we can also observe that the surface of the $(\text{Cu}_{0.9}\text{Zn}_{0.1}\text{S})$ film is composed of semi-spherical and hexagonal nanostructures; these structures consist of aggregates packed grains with other regularity arrange. The surface of the $(\text{Cu}_{0.7}\text{Zn}_{0.3}\text{S})$ film is composed of semi-spherical structures, while the surfaces of the $(\text{Cu}_{0.5}\text{Zn}_{0.5}\text{S}$, $\text{Cu}_{0.3}\text{Zn}_{0.7}\text{S}$ and $\text{Cu}_{0.1}\text{Zn}_{0.9}\text{S})$ films are composed of cauliflower-like nanostructures. **Table (3)** shows the average particle size of $\text{Cu}_x\text{Zn}_{1-x}\text{S}$ (where $x = 0, 0.1, 0.3, 0.5, 0.7, 0.9, 1$) thin films. From the table, it can be noticed that the average particle size values are (52.6) nm and (46.2) nm of CuS film and ZnS film respectively. While the average particle size of the prepared films with different mixing ratios increases with increasing of CuS ratio. The highest value of the average particle size is for $(\text{Cu}_{0.9}\text{Zn}_{0.1}\text{S})$ film with value of (47.8 nm). Similar nanostructures were previously recorded in other reports^{3,7,8,15,20}.

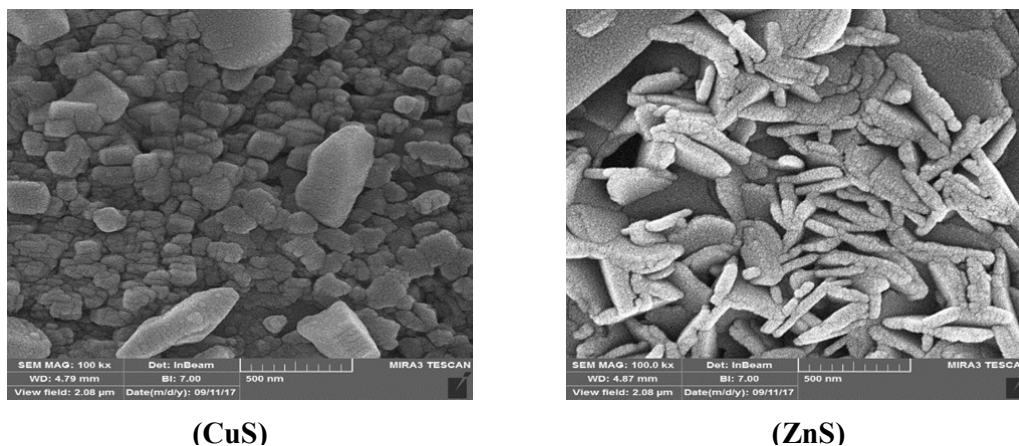
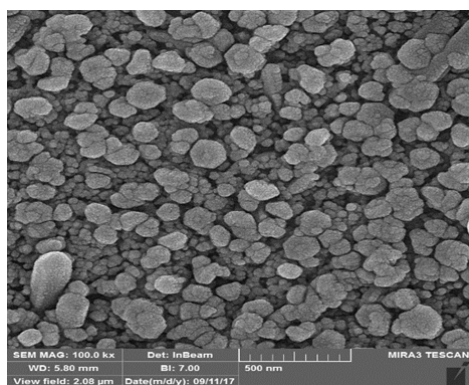
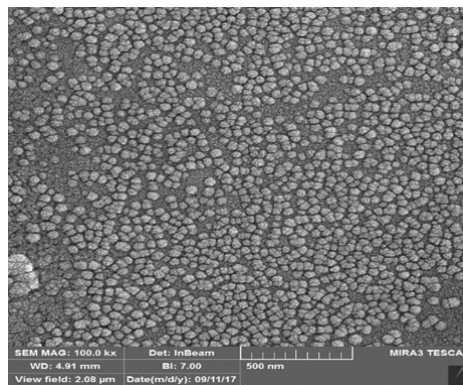
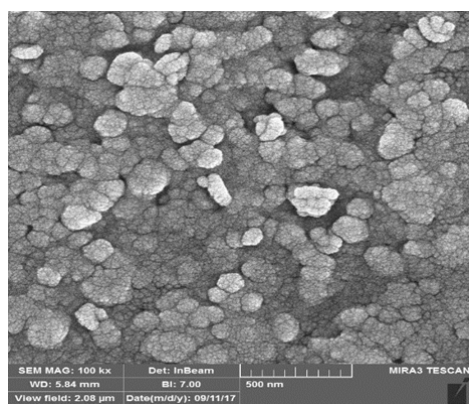
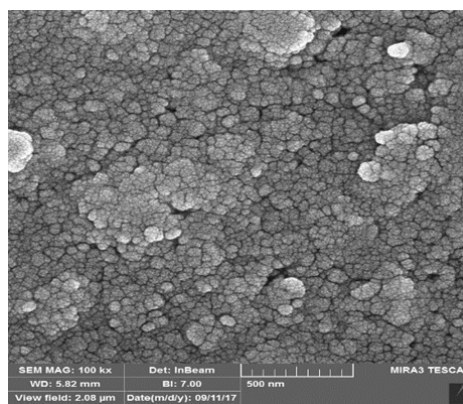
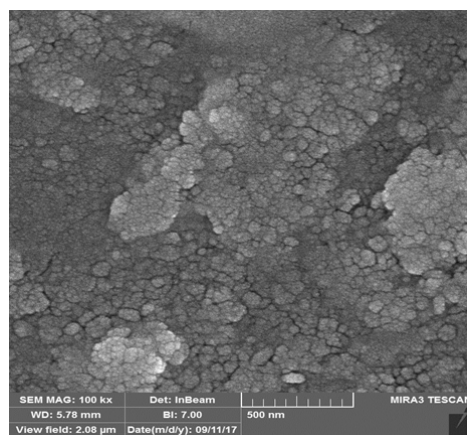


Fig. (3a): FESEM images of CuS and ZnS thin.

Table (3): Average particle size of $\text{Cu}_x\text{Zn}_{1-x}\text{S}$ thin films.

x value of $\text{Cu}_x\text{Zn}_{1-x}\text{S}$	1 (CuS)	0.9	0.7	0.5	0.3	0.1	0 (ZnS)
Particle Size (nm)	52.6	47.8	44.2	43.3	33.2	30.6	46.2

**(Cu_{0.9}Zn_{0.1}S)****(Cu_{0.7}Zn_{0.3}S)****(Cu_{0.3}Zn_{0.7}S)****(Cu_{0.5}Zn_{0.5}S)****(Cu_{0.1}Zn_{0.9}S)****Fig. (3b):** FESEM images of Cu_xZn_{1-x}S (where x= 0.9, 0.7, 0.5, 0.3 and 0.1) thin films.

3.4 Optical studies: The optical properties of the prepared thin films have been investigated by using UV-Vis-NIR spectroscopy in the region of (350-900) nm. **Figure (4)** shows the transmittance spectra as a function of the wavelength of $\text{Cu}_x\text{Zn}_{1-x}\text{S}$ (where $x=0, 0.1, 0.3, 0.5, 0.7, 0.9$ and 1) thin films. It can be noticed that the transmittance increases rapidly as the wavelength increases in the range of (350-400) nm, and then increases slowly at higher wavelengths, and we also notice that the transmittance of all prepared films decreases with the increase in x value. The maximum transmittance value is $\sim 90\%$ of ZnS thin film and the minimum transmittance is $\sim 55\%$ of CuS thin film.

The absorption coefficient (α) can be estimated from the absorbance using the formula¹⁹:

$$\alpha = (2.303 \times A)/t \quad (5)$$

Where A is the absorbance and t is the thickness of the sample. **Figure (5)** shows the relationship between the absorption coefficient and the photon energy of $\text{Cu}_x\text{Zn}_{1-x}\text{S}$ (where $x=0, 0.1, 0.3, 0.5, 0.7, 0.9$ and 1) thin films. The figure shows that the absorption coefficient increases with increasing the photon energy for all prepared thin films in the visible spectrum region. The absorption coefficient value is $>10^4 \text{ cm}^{-1}$ for all samples, which indicates that the films have direct electronic transitions. We notice from the figure that the absorption coefficient of all prepared films increases as the x value increases.

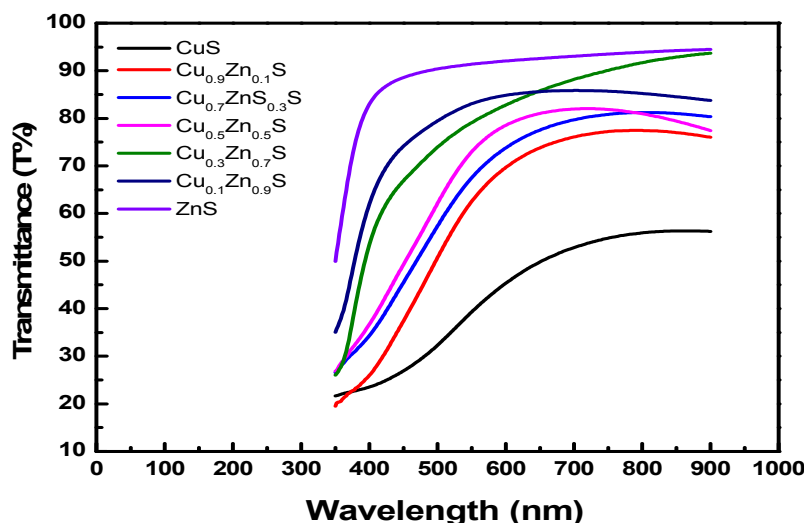


Fig. (4): The transmittance as a function of wavelength of $\text{Cu}_x\text{Zn}_{1-x}\text{S}$ thin films.

The optical energy gap (E_g) values can be calculated by using Tauc's relation¹⁵:

$$\alpha h\nu = B(h\nu - E_g)^r \quad (6)$$

Where $h\nu$ is the photon energy, B is a constant which does not depend on photon energy and r has four numeric values, (1/2) for allowed direct, 2 for allowed indirect, 3 for forbidden direct and 3/2 for forbidden indirect optical transitions. **Figure (6)** shows the plot of $(\alpha h\nu)^2$ versus $h\nu$ and the energy gap (E_g) value is calculated by using the absorption coefficient values and (Tauc's equation) by assuming allowed direct transition between valance and conduction bands.

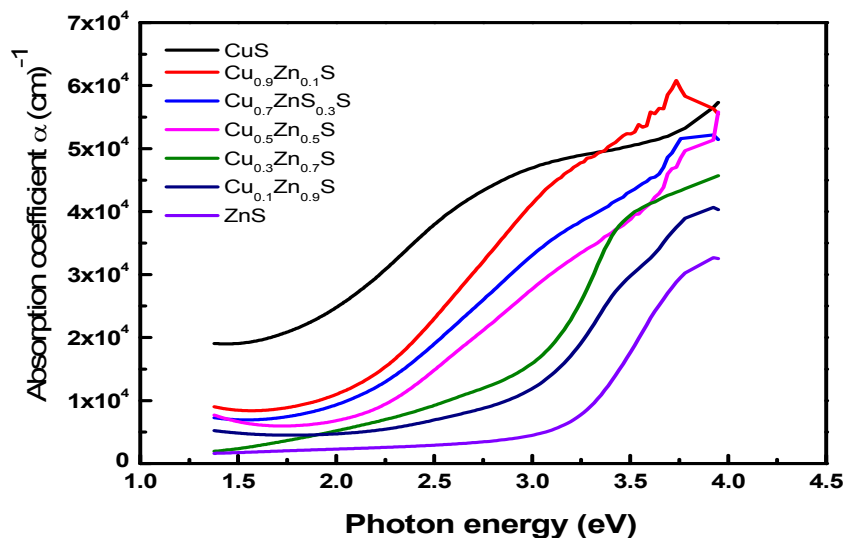


Fig. (5): The relationship between the absorption coefficient and the photon energy of $\text{Cu}_x\text{Zn}_{1-x}\text{S}$ thin films.

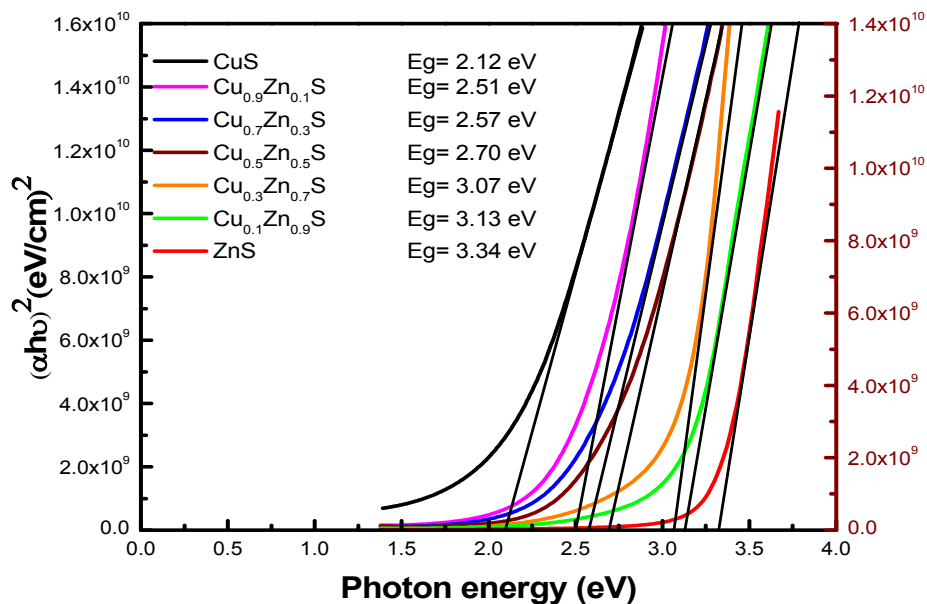


Fig. (6): The relation between $(\alpha h\nu)^2$ and $(h\nu)$ of $\text{Cu}_x\text{Zn}_{1-x}\text{S}$ thin films

We notice from the figure that the energy band gap values of the prepared thin films decrease as the x value increases, where the values are in the range of (2.12-3.34) eV. It has been proven experimentally that the copper bonding with some elements such as zinc and cadmium causes a decrease in the energy gap¹⁷.

4. CONCLUSIONS

In this study, the chemical spray pyrolysis method was used successfully for deposition of $\text{Cu}_x\text{Zn}_{1-x}\text{S}$ (where $x = 0, 0.1, 0.3, 0.5, 0.7, 0.9$ and 1) thin films on glass substrate at temperature of (400°C). From X-ray diffraction results, it is concluded that the (CuS) thin film has polycrystalline structure (covellite-hexagonal) type with preferred orientation of (103), whereas the ZnS thin film has a polycrystalline structure and (wurtzite-hexagonal) type with preferred orientation of (0010). Furthermore, other thin films prepared with different mixing ratios (x values) have a polycrystalline structures with a mixture of the two phases. The AFM results show that all films are homogeneous and smooth. The FESEM results confirmed the formation of nanostructures with different shapes and morphologies, such as cauliflower, semi-spherical, hexagonal and in the form of plates and rods. The optical measurements show that the transmittance of the prepared thin films decreases as the x value increases. It is found that the band gap decreases as the x value increases, where the values are in the range of (2.12-3.34) eV. We conclude that the structures and optical properties of the prepared thin films improved with the increase in CuS ratio (x value), suggesting that the prepared thin films can be used as an effective materials in the manufacture of optical devices.

REFERENCES

1. M. Ramya and S. Ganesan, "Annealing effects on resistivity properties of vacuum evaporated Cu_2S thin films", *Int. J. Pure and Appl. Phys.*, 2010, 6(3), 243-249.
2. E. Guneri and A. Kariper, "Optical properties of amorphous CuS thin films deposited chemically at different pH values", *J. Alloys compd.*, 2012, 516, 20-26.
3. M. Adeliford, H. Eshghi and M. B. Mohagheghi, "Synthesis and characterization of nanostructural CuS-ZnS binary compound thin films prepared by Spray Pyrolysis", *Opt. Commun.*, 2012, 285, 4400- 4404.
4. M. Kemmler, M. Lazell, P. O'Brien, D. J. Otway, J. H. Park and J. R. Walsh, "The growth of thin films of copper chalcogenide films by MOCVD and AACVD using novel single-molecule", *J. Mater. Sci.*, 2002, 13, 531-535.
5. B. Guzeldir, M. Saglam and A. Ates, "Deposition and characterization of CdS, CuS and ZnS thin films deposited by SILAR method", *Acta Phys. Pol. A*, 2012, 121, 33-35.
6. Y. Lu, X. Meng, G. Yi and J. Jia, "In situ growth of CuS thin films on functionalized self-assembled monolayers using chemical bath deposition" *J. Colloid Interface Sci.*, 2011, 356, 726-733.
7. M. Xin, K. Li and H. Wang, "Synthesis of CuS thin films by microwave assisted chemical bath deposition", *Appl. Surf. Sci.*, 2009, 256, 1436-1442.
8. K. J. Wang, G. D. Li, J. X. Li, Q. Wang and J. S. Chen, "Formation of single-crystalline CuS nanoplates vertically standing on flat Substrate", *Cryst. Growth Des.*, 2007, 7, 2265-2267.
9. K. Priya, V. K. Ashith, G. K. Roa and G. Sanjeev, "A comparative study of structural, optical and electrical properties of ZnS thin films obtained by thermal evaporation and SILAR techniques", *Ceram. Int.*, 2017, 43, 10487-10493.
10. Y. Tamomura, M. Kitagawa, A. Suzuki and S. Nakajima, "Homoepitaxial growth of ZnS single crystal thin films by molecular beam epitaxy", *J. Cryst. Growth*, 1990, 99, 451-454.

11. P. J. Dean, A. D. Pitt, M. S. Skolnick, P. J. Wright and B. Cockayne, "Optical properties of undoped organometallic grown ZnSe and ZnS", *J. Cryst. Growth*, 1982, 59, 301-306.
12. Z. Y. Zhong, E. S. Cho, and S. J. Kwon, "Characterization of the ZnS thin film buffer layer for Cu(In, Ga)Se₂ solar cells deposited by chemical bath deposition process with different solution concentrations", *Mater. Chem. Phys.*, 2012, 135, 287-292.
13. H. M. Hennayaka and H. S. Lee, "Structural and optical properties of ZnS thin film grown by pulsed electrodeposition", *Thin Solid Films*, 2013, 548, 86-90.
14. A. S. Fathima, N. Sivaguru and V. S. Kumar, "Investigation on optical properties of CuS thin films by chemical bath deposition", *IOSR- J. Appl. Phys.*, 2016, 4, 13-16.
15. W. Daranf, M. S. Aido, A. Hafdallah and H. Lekiket, "Substrate temperature influence on ZnS thin films prepared by ultrasonic spray", *Thin Solid Films*, 2009, 518, 1082-1084.
16. S. MuthuKumaran and M. A. Kumar, "Structural, fir and photoluminescence properties of ZnS:Cu thin films by chemical bath deposition method", *Mater. Lett.*, 2013, 93, 223-225.
17. H. S. AL-Jumaili, M. H. Suhail and W. Bedeawy, "Preparation and studying some physical properties of Zn: Cd: S: Cu quaternary structure thin film by chemical spray pyrolysis", *Journal of Al- Anbar University for Pure Science*, 2006 ,1, 1, 1-13.
18. B. Cullity and S. Stock, *Elements of X-ray Diffraction*, 3rd Edition, Princeton Hall, United States, 2001.
19. N. A. Bakr, Z. T. Khodair, and A. M. Shano, "Effect of aqueous solution molarity on structural and optical properties of Ni_{0.92}Co_{0.08}O thin films prepared by chemical spray pyrolysis method", *Int. J. Thin. Fil. Sci. Tec.*, 2015, 4, 2, 111-119.
20. S. S. Dhasade and J. S. Fulari, "Synthesis of CuS nanorods grown at room temperature by electrodeposition method", *Mater. Chem. Phys.*, 2012, 137, 353-358.

***Corresponding Author: Nabeel A. Bakr**

Department of Physics, College of Science, University of Diyala, Diyala, Iraq

Online Publication Date: 18.01.20187